



Fire risk, atmospheric chemistry and radiative forcing assessment of wildfires in eastern Mediterranean

E. Athanasopoulou ^{a,*}, D. Rieger ^b, C. Walter ^b, H. Vogel ^b, A. Karali ^a, M. Hatzaki ^a, E. Gerasopoulos ^a, B. Vogel ^b, C. Giannakopoulos ^a, M. Gratsea ^a, A. Roussos ^a

^a Institute for Environmental Research and Sustainable Development (IERSD), National Observatory of Athens (NOA), Lofos Koufou, GR 152 36, P. Penteli, Athens, Greece

^b Institute for Meteorology and Climate Research, Karlsruhe Institute of Technology (KIT), Postfach 3640, D-76021, Karlsruhe, Germany



HIGHLIGHTS

- Fire danger forecasting by COSMO-ART is proven.
- Forest burning results to tripled AOD values (0.75–1) than these in non-fire periods.
- Fires contribute around 50% to the total PM₁₀, 60 km downwind fire spots (Athens).
- The radiative impact of fire-induced aerosol is negative (3-day-average of -10 W m^{-2}).
- The effect of fire plume on air temperature is $-0.5/-5 \text{ K}$ (3-day-average/hourly value).

ARTICLE INFO

Article history:

Received 12 March 2014

Received in revised form

27 May 2014

Accepted 30 May 2014

Available online 5 June 2014

Keywords:

Wildfires

Fire weather index

Organic carbon

Elemental carbon

Aerosol radiative forcing

Greece

ABSTRACT

The current research study aims at investigating the atmospheric implications of a major fire event in the Mediterranean area. For this purpose, a regional aerosol model coupled online with meteorology (COSMO-ART) is applied over Greece during late summer 2007. Fire risk model results proved to be adequate in reproducing the highly destructive event, which supports further applications for national meteorological forecasts and early warning systems for fire prevention. Columnar aerosol loading field predictions are consistent with satellite maps, which further allows for the correlation of this wildfire event to the atmospheric chemistry and the radiative forcing. Gaseous chemistry resembles that in urban environments and led to nitrogen dioxide and ozone exceedances in several cities in proximity to and downwind the fire spots, respectively. Influence in Athens is found significant from the Euboean plume (45% of total surface PM₁₀) and small (5%) from the fires in Peloponnese. Fire events are indicated by sharp increases in organic to elemental carbon (6), together with sharp decreases in secondary to total organic components (0.1), in comparison to their values during the pre- and post-fire period over Athens (1 and 0.6, respectively). The change in the radiative budget induced by the fire plume is found negative (3-day-average value up to -10 W m^{-2}). Direct heat input is found negligible, thus the net temperature effect is also negative over land (-0.5 K). Nevertheless, positive temperature changes are found overseas (hourly value up to $+2 \text{ K}$), due to the amplified radiation absorption by aged soot, coupled to the intense stabilization of the atmosphere above the sea surface.

© 2014 Elsevier Ltd. All rights reserved.

1. Introduction

An average of 50,000 fires sweep away from 700,000 to 1,000,000 ha of the Mediterranean forests per annum (FAO, 2007), following an increasing trend during the last decades and causing

enormous economic and ecological destruction. Greece has the most severe forest fire problems among the European Union countries (EU, 2001; Moriondo et al., 2006). It has been estimated that the average area burnt per fire is 3940 ha in Greece, 2847 ha in Spain, 1974 in Italy and 1529 in Portugal (Iliadis et al., 2002).

The link between wildfire occurrence and climatic variables is widely studied (Pereira et al., 2002; Bassi et al., 2008; Carvalho et al., 2008; Founda and Giannakopoulos, 2009). The current climate change trend in the Mediterranean causes longer summer

* Corresponding author.

E-mail address: eathan@meteo.noa.gr (E. Athanasopoulou).

droughts and intensification of these droughts even out of season. As a result, the frequency of large-scale forest fires is on the rise. When a period of drought and high temperatures is followed by a day of peak temperatures, low relative humidity and very strong winds, fire danger reaches extreme levels and multiple fires can easily get out of control creating havoc. The contribution of these meteorological factors to fire risk can be estimated by several non-dimensional indices of fire risk, such as the Mc Arthur Forest Fire Danger Index used in Australian forests (Mc Arthur, 1967), the Fire Weather Index (FWI) developed in Canada (Van Wagner, 1987) and the Finnish Fire Index (Venäläinen and Heikinheimo, 2003).

Wildfires have serious short- and long-term impacts on human health. One of the main relevant aspects is their significant contribution to elevated PM₁₀ concentrations (e.g. Bytnerowicz, 2009; Pio et al., 2008). In particular, organic aerosol over Athens presented a tenfold increase during the wildfires of 2009 (Amiridis et al., 2012). Aerosol modeling studies of the Greek wildfires of 2000 and 2007 and of the fire seasons of 2003, 2004 and 2005 in Portugal have found similar fire-induced effects (Lazaridis et al., 2008; Hodnebrog et al., 2012; Martins et al., 2012; Poupkou et al., 2013). Concerning gases, fire emissions (nitrogen oxides, hydrocarbons etc) provoke ozone titration near the source, but are positive contributors downwind, enhancing ozone production (Kouvarakis et al., 2002; Bossoli et al., 2012; Strada et al., 2012).

During important fire events, the radiative impact on a regional scale could be quite significant. At the surface, for both clear and total sky conditions, the predominant radiative forcing is negative. This is mainly due to the increased scattering and absorption of shortwave flux by the carbonaceous aerosol. These effects have been studied over Europe, Asia and Russia for the wildfire periods of 2003, 2008 and 2010 respectively and in boreal North America for an extended time series (Hodzic et al., 2007; Natarajan et al., 2012; Jin et al., 2012; Pérez et al., 2014). Their results indicate that fires reduce surface net radiation considerably (up to 80–150 W m⁻² in diurnal-averaged). An exception occurred for Europe during the fire period of 2003, when a positive daily averaged radiative forcing (up to +40 W m⁻²) is found (Hodzic et al., 2007).

This study aims at investigating the issues addressed above, by applying the regional atmospheric online-coupled model COSMO-ART (Vogel et al., 2009). In specific, the objectives of this work are to: (a) investigate the potential of fire danger forecasting, (b) estimate the footprint of the wildfires in terms of air quality and atmospheric chemistry, (c) estimate the direct radiative impact, (d) calculate the direct heat input and estimate subsequent net temperature impacts and (e) use the above to evaluate the model and its application in the eastern Mediterranean.

2. Methodology

2.1. Model framework

COSMO-ART is a regional chemistry transport model (ART stands for Aerosols and Reactive Trace gases) online-coupled to the COSMO regional numerical weather prediction and climate model (Baldauf et al., 2011). As a fully online-coupled model it allows for feedbacks of aerosols on temperature, radiation and cloud condensation nuclei (CCN) (Vogel et al., 2009; Bangert et al., 2011; Athanasopoulou et al., 2013). Analytical description of the treatment of different components and processes is provided in the Supplement (Section S1).

In the frame of the current study, the direct heat input of forest fires is incorporated to the model. To this end, the fire radiative power (FRP) effect on temperature is incorporated as a separate term into the total temperature tendency (Doms et al., 2011). All equations are provided in the Supplement (Section S2).

2.2. Model setup

The base-case simulation for the current study is performed between August 15 and September 13, 2007, over an area extending from 33.6 to 41.8 °N and from 18.5 to 29.5 °E (Fig. 1a), with the fine horizontal resolution of 0.025° (around 2.8 km) and a vertical extend up to 20 km covered by 40 layers, with the first being approximately 20 m thick. Interpolated initial and boundary meteorological data, updated every 3 h are driven by a coarse-grid (7 km) COSMO model application. Boundary data for gas-phase are retrieved by the global model MOZART (Emmons et al., 2010) with an update frequency of 6 h, while boundary concentrations for aerosol species are described in Athanasopoulou et al. (2013). More information on the gas-phase, aerosol and meteorological inputs is provided in the Supplement (Section S1).

Apart from the base-case simulation, a series of additional scenarios is applied (Table 1). Scenario 1 is a simulation without wildfire emissions. It uses the same configuration with the base-case application and their differences reveal the role of the wildfires on aerosol chemistry (Section 3.3), as well as their direct radiative forcing during summer 2007 (Section 3.5).

Scenario 2 implements the direct heat input of forest fires into COSMO-ART and it investigates the subsequent temperature changes (Section 3.5). It uses the same configuration with the base-case application.

Scenario 3 is a simulation incorporating Saharan dust production. The necessity for this scenario was the concurrent Saharan dust intrusion over Greece (20 August – 03 September, 2007). For this scenario the model is applied for an area extending from 10 to 44 °N and from 20 °W to 31.5 °E, with a horizontal resolution of 0.25° (around 28 km). The meteorological initial and boundary conditions are obtained by the GME global model, as described in the Supplement (Section S1). Surface dust concentrations and optical depth data from scenario 3 are combined with the base-case outputs when compared with measurements (Sections 3.2 and 3.4).

A model inter-comparison is presented in Section 3.2 between COSMO-ART (scenario 3) and BSC-DREAM8b model v2.0. Description of this model can be found in several publications (Pérez et al., 2006a; 2006b; Basart et al., 2012). The parameter compared is the aerosol optical depth of dust (AOD, at the wavelength of 550 nm).

2.3. Emissions

The anthropogenic emissions implemented in COSMO-ART simulations are based on the TNO/MACC inventory (Kuenen et al., 2011), while, in the frame of the current study, wildfire emissions are retrieved from the Global Fire Emissions Database (GFED) version 3 (Van der Werf et al., 2010). More information on emissions is found in the Supplement (Section S3 and S4).

The important fire periods in Greece during late summer 2007, according to the GFED database, are shown in Table 1. By comparing the spatial distribution of fire emissions with the location of fire spots, as identified from satellites (red points in Fig. 1b) and from wildfire detection studies (Sifakis et al., 2011; San-Miguel-Ayanz et al., 2013), it is shown that GFED data are consistent with most fire spots, but their coarse spatial resolution results in the homogeneous distribution of wildfire emissions over an expanded area (Fig. 1c). Fig. 1d shows the spatial distribution of hourly total organic carbon (OC) emissions at high anthropogenic pollution conditions. As evident, hourly emission rates over the city of Athens range between 0.1 and 2 g h⁻¹ km⁻², while fire emissions are higher more than an order of magnitude (up to 30 g h⁻¹ km⁻²).

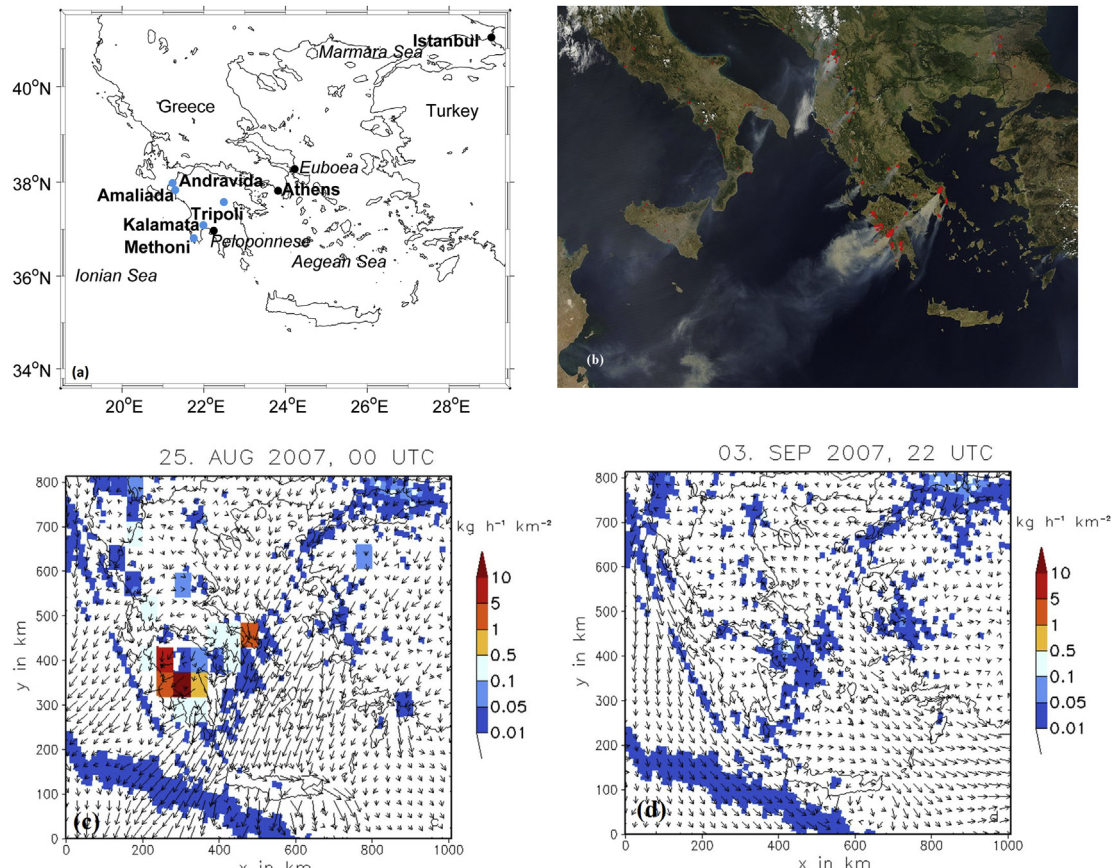


Fig. 1. Geographical maps of: (a) model domain for base-case application and scenarios 1, 2, (b) MODIS aboard Aqua image of smoke from fires in Greece, 25 August 2007 (12:05 UTC) (<http://rapidfire.sci.gsfc.nasa.gov>). (c) spatial distribution of total OC hourly emission rates ($\text{kg h}^{-1} \text{km}^{-2}$) over Greece, 25 August 2007 (22:00 UTC), and (d) same as c, but for 09 September 2007 (09:00 UTC). Meteorological monitoring sites are shown in blue and belong to the Hellenic National Meteorological Service (Andravida: $37^{\circ} 55' \text{N } 21^{\circ} 17' \text{E}$, Kalamata: $37^{\circ} 04' \text{N } 22^{\circ} 10' \text{E}$, Methoni: $36^{\circ} 50' \text{N } 21^{\circ} 42' \text{E}$, Tripoli: $37^{\circ} 32' \text{N } 22^{\circ} 24' \text{E}$) and to the National Observatory of Athens (Amaliada: $37^{\circ} 48' 09'' \text{N } 21^{\circ} 19' 44'' \text{E}$). The fire spots are shown in red. The rest indicate areas discussed within text. (For interpretation of the references to colour in this figure legend, the reader is referred to the web version of this article.)

2.4. Fire weather index

In order to investigate changes in fire risk in relation to the meteorological conditions in the area of Peloponnese, the Canadian Fire Weather Index (FWI) is applied (Van Wagner, 1987). The calculation of the index depends solely on daily noon measurements of dry-bulb temperature, air relative humidity, 10 m open wind speed and 24 h accumulated precipitation. More information on the FWI is provided in the supplement (Section S5).

Although this index has been developed for Canadian forests, its suitability has been proven for the Mediterranean region (Moriondo et al., 2006). Its adaptation and optimization for Greece was performed by Karali et al. (2014). According to this study, three critical fire risk threshold values were established based on daily mean meteorological data: FWI = 15, 30 and 45, increasing from the north-west to the south-east. For the current study, FWI is calculated using the meteorological data described below and in the Supplement (Section S6), and it is compared to FWI predictions from the standard COSMO-ART application (Section 3.1).

2.5. Measurements

Available meteorological data include daily noon (at UTC) values of temperature at 2 m above ground level (agl) (regarded as the maximum daily value), atmospheric relative humidity at 2 m agl (regarded as the minimum daily value), wind speed at 10 m agl and total daily precipitation. Air quality data include PM₁₀

concentration values and AOD (ground and satellite) retrievals. All stations are shown in Fig. 1a, while extended information on the sites and origin of measurements is provided in the Supplement (Section S6).

3. Results and discussion

Greece experienced an extreme summer and the worst natural hazard in its modern history during 2007 (Founda and Giannakopoulos, 2009). Soil dehydration, following a prolonged dry period in combination with hot and strong winds yielded favorable conditions for the ignition and spread of wildfires (Fig. S1). During the last week of August, 55 simultaneous large fires burnt 170,000 ha in the Peloponnese region and 25,000 ha in the Euboea island, which corresponded to 70% (approximately 3,300,000 ha) of the total burnt area in the country during all years, and to 55% (approximately 500,000 ha) of the total burnt area across south Europe during 2007 (Bassi et al., 2008; European Commission, 2008; San-Miguel-Ayanz et al., 2013). More information on the synoptic and weather conditions during summer 2007 can be found in the Supplement (Section S7).

3.1. Meteorological and fire risk values from simulations and observations

The day-by-day variation of the predicted and observed FWI during the examined event (15/8–13/9/2007) is presented in Fig. 2.

Table 1

Description of modeling scenarios performed by the current COSMO-ART application.

Scenario	Simulation period (2007)	Scenario's description	Objective	Other information
Base-case	15 August – 13 September	Standard wildfire simulation ^a	Wildfire effects over Greece	21 August – 3 September: fire period in Peloponnese; 24–29 August: fire period in Euboea
1	15 August – 13 September	zero wildfire emissions ^a	Wildfire aerosol chemistry and feedbacks on radiation and temperature	–
2	25–27 August	direct heat input of wildfires to air temperature ^a	Wildfire radiative power feedbacks on temperature	Peak fire period in Peloponnese and in Athens
3	20 August – 3 September	Saharan dust production ^b	Saharan dust intrusion over Greece	–

^a The simulation area extends from 33.6 to 41.8 N and from 18.5 to 29.5 E (Greece, zero dust emissions), horizontal resolution of 0.025°, COSMO initialization.

^b The simulation area extends from 10 to 44 °N and from 20 °W to 31.5 °E, horizontal resolution of 0.25°, GME initialization.

For each station, the observed average FWI for the entire fire season, namely from May to October 2007, is calculated and ranges between 30 and 45 (red line in Fig. 2). Monthly mean values of the basic meteorological parameters and the FWI together with performance metrics are shown in Table S1 and discussed. It should be noted that precipitation during the examined event was negligible or zero, so the metrics for the model performance in relation to precipitation are not calculated.

The FWI variation is well captured by the model at all five sites in Peloponnese. Specifically, the predicted as well as the observed FWI values are above the average during the fire season, reaching their peak values (above 50) during the peak fire period. According to a recent analysis of large fires, this event is characterized by the highest FWI values in the Mediterranean during 2003–2013 (San-Miguel-Ayanz et al., 2013).

During September, the predicted and the observed FWI values are closer to the average of the fire season except for the Methoni station. The most striking deviations between the predicted and observed values are during August, 24–25 and September, 2–5, but without stemming from a systematic model behavior.

In particular, FWI is overestimated in Amaliada and Methoni during 24–25 August, but for different reasons (wind speed overestimations and relative humidity underestimations, respectively), while it is underestimated in Andravida and Kalamata, caused by the inverse model discrepancies (relative humidity overestimations and wind speed underestimations, respectively). During 2–5 September, deviations in wind speed resulted in FWI overestimations in Amaliada and Andravida, and underestimations in Tripoli, Methoni and Kalamata. Overestimations of the atmospheric relative humidity contributed to the lower FWI model estimations at the site of Kalamata.

Air temperature is generally well estimated, thus it does not significantly contribute to FWI model discrepancies. Exceptions occur on August, 23 at Amaliada (overestimated T and FWI), on August, 24 and 25 at Methoni and on September, 2 at Methoni and Kalamata (underestimated T and FWI).

Precipitation occurred only on September, 7 and 12 over Kalamata, where light rainfall was measured but not predicted. This significantly contributed to a higher predicted fire risk than estimated by measurements.

Overall, the predicted temperature and humidity are highly correlated with the corresponding observed values, while weaker, though statistically significant correlations are found for wind speed (except for Kalamata). The differences between mean observations and predictions for all parameters at all sites are not statistically significant at the 95% confidence level ($\alpha = 0.05$), according to the two-sample *t*-test, except for wind speed at Amaliada and Methoni and relative humidity at Methoni. The root mean square errors (RMSE) indicate that the average magnitude of the errors is of the same order among the sites for all parameters. Wind

speed and FWI are generally overestimated by the model, as shown by the mean normalized biased (MNB). Specifically, the statistically significant wind speed overestimation in one site (Amaliada) is also reflected on the FWI values.

In summary, increased fire risk is found during summer 2007 in Peloponnese, as revealed by the FWI from both observations and model predictions. The peak values of the FWI coincided the timing of the actual fire event, depicting the significant role of meteorological conditions on the ignition of the fires. Model discrepancies are non-systematic and stem mainly from wind speed deviations (both under- and overestimations) and/or relative humidity overestimations. Nevertheless, COSMO-ART FWI predictions proved to be adequate in reproducing the highly destructive event.

3.2. Comparison between AOD fields from simulations and observations

The COSMO-ART's aerosol performance during the examined event is assessed by comparing predicted fields of the columnar aerosol load (AOD) against the respective satellite maps. AOD from COSMO-ART is provided as type-specific: representative of the sea-salt modes with diameters from 0.02 to 28 μm (AOD_{sea}, at the wavelength of 550 nm), of the dust modes with diameters from 1 to 20 μm (AOD_{dst}, at the wavelength of 550 nm) and of the sum of all other aerosol (including fire-induced) in the submicron size range and (AOD_{SM}, at the wavelength range of 250–700 nm).

The first period selected for the study of aerosol distribution over the simulation domain is that of the pre-wildfire days (17–20 August, Fig. 3a, b). Aerosol loadings over Peloponnese can be regarded as the background regime and are measured around 0.25. It is encouraging that all aerosol peak areas are captured by the base-case simulation. A source of model underestimation is the size range of the modeled aerosol loading by this scenario (AOD_{SM}), in comparison to the total aerosol optical depth measured. Indeed, the aerosol fine mode fraction for AOD is measured around 0.3 over Peloponnese, 0.5 over Athens and up to 0.7 over Thessaloniki (fig. S2a).

During the next four days (21–24 August, Fig. 3c, d), the ability of the model to reproduce several non-urban sources of aerosol loadings is tested. The first tongue of the Saharan dust intrusion occurs over the central Mediterranean. The source of dust mobilization, as depicted from both observations and the model, is the heart of the Sahara in Mali and Mauritania, known as one of the major source regions of dust particles (Engelstaedter and Washington, 2007; Israelevich et al., 2002), which are being transported towards the Eastern Mediterranean via the Gulf of Tunis (Gerasopoulos et al., 2011). Along this path of transport, high AOD values (up to 1) are found in both the COSMO-ART outputs and the satellite retrievals.

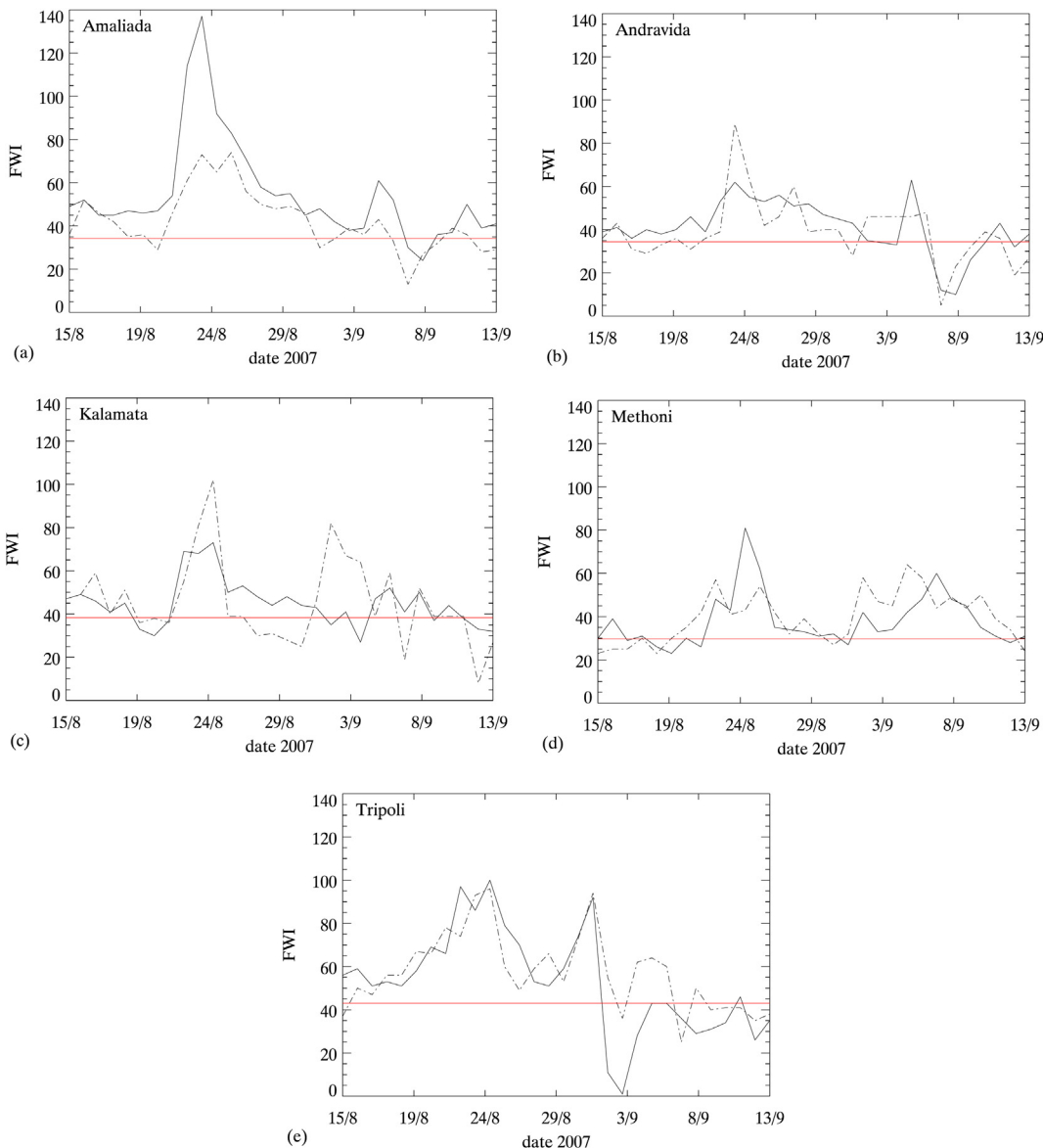


Fig. 2. Time evolution between 15 August – 13 September, 2007, of the FWI over (a) Amaliada, (b) Andravida, (c) Kalamata, (d) Methoni, and (e) Tripoli. FWI values are calculated from observations (dashed line) and COSMO-ART predictions (solid line). Red lines correspond to the observed average FWI value for the 2007 fire season. Sites are shown in Fig. 1a. (For interpretation of the references to colour in this figure legend, the reader is referred to the web version of this article.)

The origin of elevated aerosols over the Atlantic is mainly sea-salt production, according to the AOD_{sea} model output (fig. S3a). The highest aerosol loadings are predicted at the coastline of Northern Africa and are found a mixture of types: anthropogenic sources produce the largest quantities (AOD_{SM} is up to 0.7, fig. S3c), while dust and sea-salt particles are contributing almost equally to the local aerosol burden (AOD_{dst} and AOD_{sea} values are around 0.3, fig. S3a and b). Model peaks are higher than satellite retrievals both for dust and sea-salt. Uncertainties in the dust source functions within aerosol models are common, and are usually treated by model tuning in respect to observations, but this is outside the scope of the current study. Concerning AOD_{sea} , the overestimation of sea-salt mass concentrations during high winds and increased sea-salt production, is explained by the stronger flux-wind speed relationship of Mårtensson et al. (2003) (Ovadnevaite et al., 2013), which is also used by COSMO-ART (Lundgren et al., 2013).

The next averaged period corresponds to the peak fire period over Peloponnese (Fig. 3e, f). High AOD values are captured by both

products over an extended area downwind the fire spots. In specific, aerosol loadings over Peloponnese are found tripled (AOD is around 0.75) when compared with the non-fire period. The higher values (AOD_{SM} up to 1) and spatial variability of predictions are related to the better spatial resolution of the base-case run (0.025°) in comparison to the satellite image (1°).

The last period (1–6 of September 2007, Fig. 3g, h) assesses AOD predictions under anthropogenic influence. Peaks over northern Greece and north-west Turkey are found around 0.65 both from COSMO-ART and MODIS and correspond to urban, industrial and maritime activities around and downwind of Thessaloniki, Istanbul and over the gulf of Marmara. According to dust predictions from scenario 3 (Fig. 4a), Saharan dust is still over Greece during the two latter periods, which is largely why the base-case simulation cannot reproduce the background AOD values observed over the rest of the domain. Aerosol loadings in the coarse mode, which are not captured by the base-case scenario (AOD_{SM}), add to this underestimation. Indicatively, the predicted aerosol load is expected

to underestimate total AOD measurements by about 60–80% over the greater Athens area during this period (Fig. S2c).

In order to examine the higher temporal resolution signals (diurnal course) of different aerosol types, a time series of modeled AOD values is examined against the respective sensor retrievals (Fig. 4a). Area plots correspond to dust AOD predicted by the DREAM (dark gray) and COSMO-ART (light gray) models. Blue lines (in the web version) represent AOD values from the base-case (no dust, continuous line) and scenario 3 (dust included, dotted line). (MODIS retrievals are shown with the black line, while the) Columnar dust loadings extracted from the two models show largely the same temporal evolution of the dust event. Two primary peaks are identified (21 August and 31 August – 1 September) and shape dust optical thickness values around 0.2 (COSMO-ART value) – 0.3 (DREAM value). The effect of wildfires in Athens (see Fig. 7 and Section 3.4) is reflected mainly on the Aug. 27, shaping the total AOD value around 0.2. AOD peaks (values above 0.5) are measured during local pollution episodes (19–20 August and 2–3 September, 2007, respectively). Unlike the first episode, the second is nicely captured by COSMO-ART. Overall, the squared correlation coefficient ($r^2 = 0.57$) indicates a reasonable representation of aerosol load by COSMO-ART (Fig. 4b). Indeed, more than 85% of the data points for AOD lay within the 1:2 and 2:1 error lines.

3.3. Wildfires and atmospheric chemistry

Fig. 5 depicts the spatial distribution of the fire-induced gaseous (nitrogen oxides: NO_x and ozone: O_3) and aerosol carbon species averaged over the peak fire period. Most fire spots are situated in Peloponnese, but fires ignited also in several parts in Euboea, greatly influencing the greater Athens area (see next section) due to the strong north-eastern winds. Representative sites of these areas are selected in order to study the daily variation of pollution (Fig. 6).

As shown in both figures, ozone behavior over fire-spots resembles that in urban environments, i.e. the emission of NO_x and non-methane hydrocarbons during the fire event, determines O_3 balance in the area. NO_x emissions resulted to high ambient concentrations (80–100 ppb, shown in Fig. 5a) over the fire spots that in turn led to O_3 removal via titration (15–35 ppb, shown in Fig. 5b). Downwind the fires, NO_x levels were much lower (<30 ppb) and O_3 is accumulated (50–70 ppb). The same occurs over the fire spots, before and after the extreme burning. Similar O_3 levels and behavior were also observed over the Aegean Sea, Greece, during July 2000, under high NO_x due to fresh burning (Kouvarakis et al., 2002). O_3 titration also takes place in the vertical and up to an altitude of 300 m, above which O_3 changes become again positive (Fig. 5c).

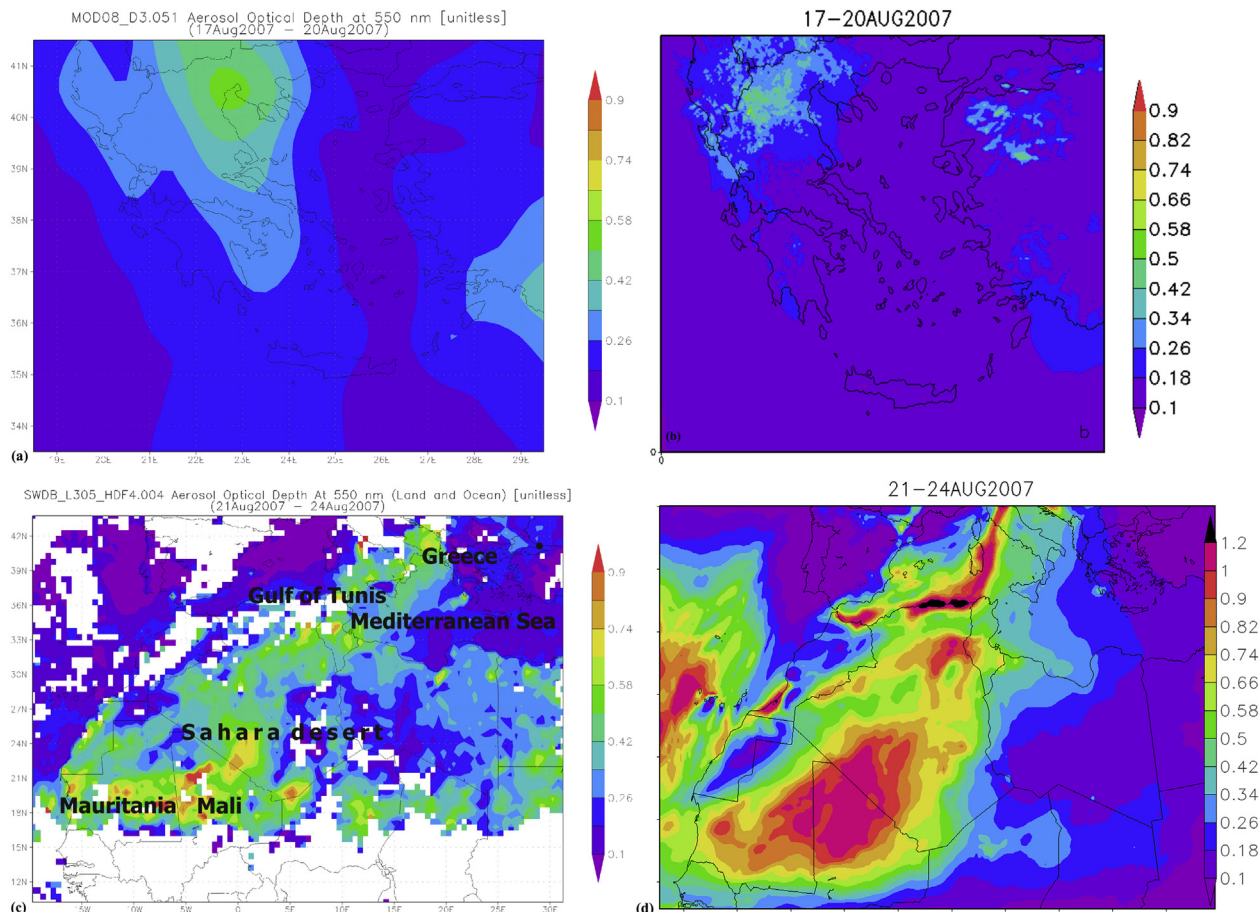


Fig. 3. Columnar aerosol load, expressed as aerosol optical depth (AOD) fields at the wavelength of 550 nm over Greece on 2007, extracted from the: (a) MODIS satellite and (b) COSMO-ART (base-case scenario), both averaged for 17–20 August, (c) SeaWiFS satellite and (d) COSMO-ART (scenario 3), both averaged for 21–24 August, (e) MODIS satellite and (f) COSMO-ART (base-case scenario), both averaged for 25–27 August, (g) MODIS satellite and (h) COSMO-ART (base-case scenario), both averaged for averaged for 1–6 September. All satellite products are total AOD values. All COSMO-ART products from the base-case application are submicron AOD (AOD_{SM}), except for scenario 3, which is the sum of dust sea-salt and rest AOD values (AOD_{dst} , AOD_{sea} and AOD_{SM} , respectively).

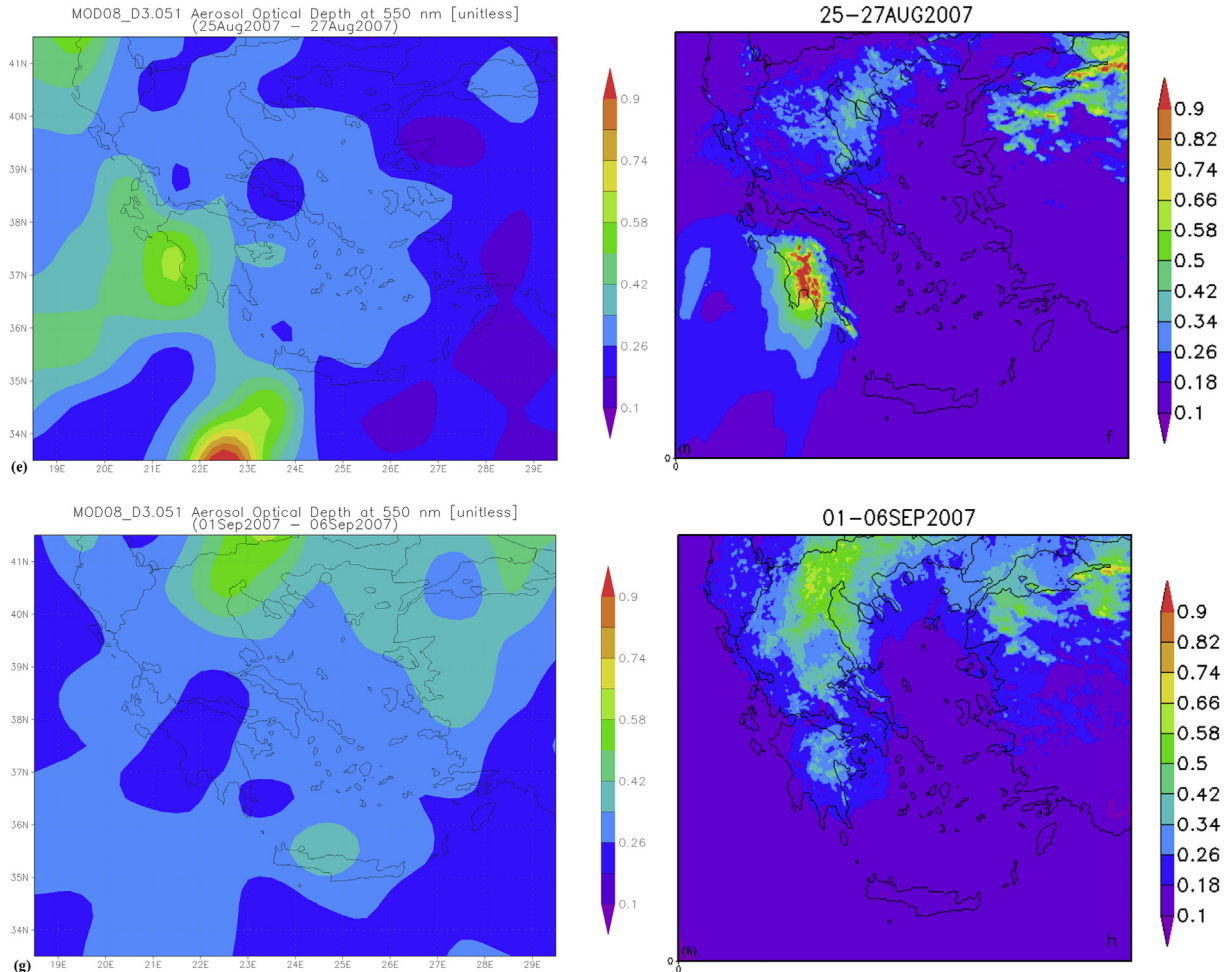


Fig. 3. (continued).

During this episode at Peloponnese, the EU air quality standards for NO_2 and O_3 were violated due to fires. In particular, NO_2 hourly values exceeded the hourly limit value of $200 \mu\text{g m}^{-3}$ for 5–17 times in the area and southern of the cities of Andravida and Amaliada, with the permitted exceedances per year set to 18. Concerning O_3 , the daily limit of 60 ppb was not exceeded close to, but further downwind fire spots (e.g. at Methoni on August, 27 and 29).

Concerning changes in aerosol species, OC increases 15 to 60 times over fire spots (Euboea and Peloponnese, respectively, shown in Fig. 6a and b), which is analogous to the area burned, fire activity, and plant productivity (Van der Werf et al., 2010). The fire plume

that reached Athens (about 60 km downwind the fire spots in Euboea) increased OC approximately 5 times (Fig. 6c). Although no OC measurements exist for this period over Athens, the daily average value of $15 \mu\text{g m}^{-3}$ estimated by COSMO-ART is similar to the daily averaged OC measurements (around $14 \mu\text{g m}^{-3}$) over Athens during the wildfires of Attica during 2009 (Amiridis et al., 2012) and the week-averaged OC measurements (around $9 \mu\text{g m}^{-3}$) downwind the fires in Portugal during 2003 (Pio et al., 2008).

Fire events are indicated by sharp increases in organic to elemental carbon (OC/EC), together with sharp decreases in

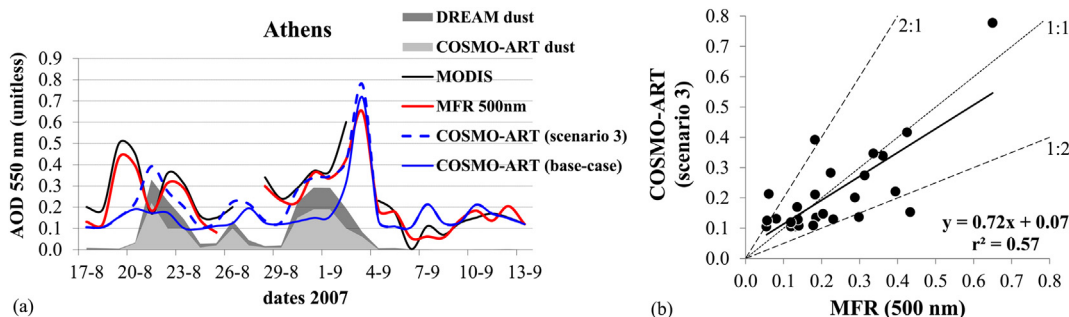


Fig. 4. Aerosol Optical Depth (AOD) from observations and predictions over Athens (site shown in Fig. 1a). ‘DREAM dust’ and ‘COSMO-ART dust’ refer to AOD_{dst} from the DREAM and COSMO-ART (scenario 3) models, respectively. ‘MODIS’ and ‘MFR’ are the products from the respective sensors (at the wavelengths of 550 and 500 nm, respectively).

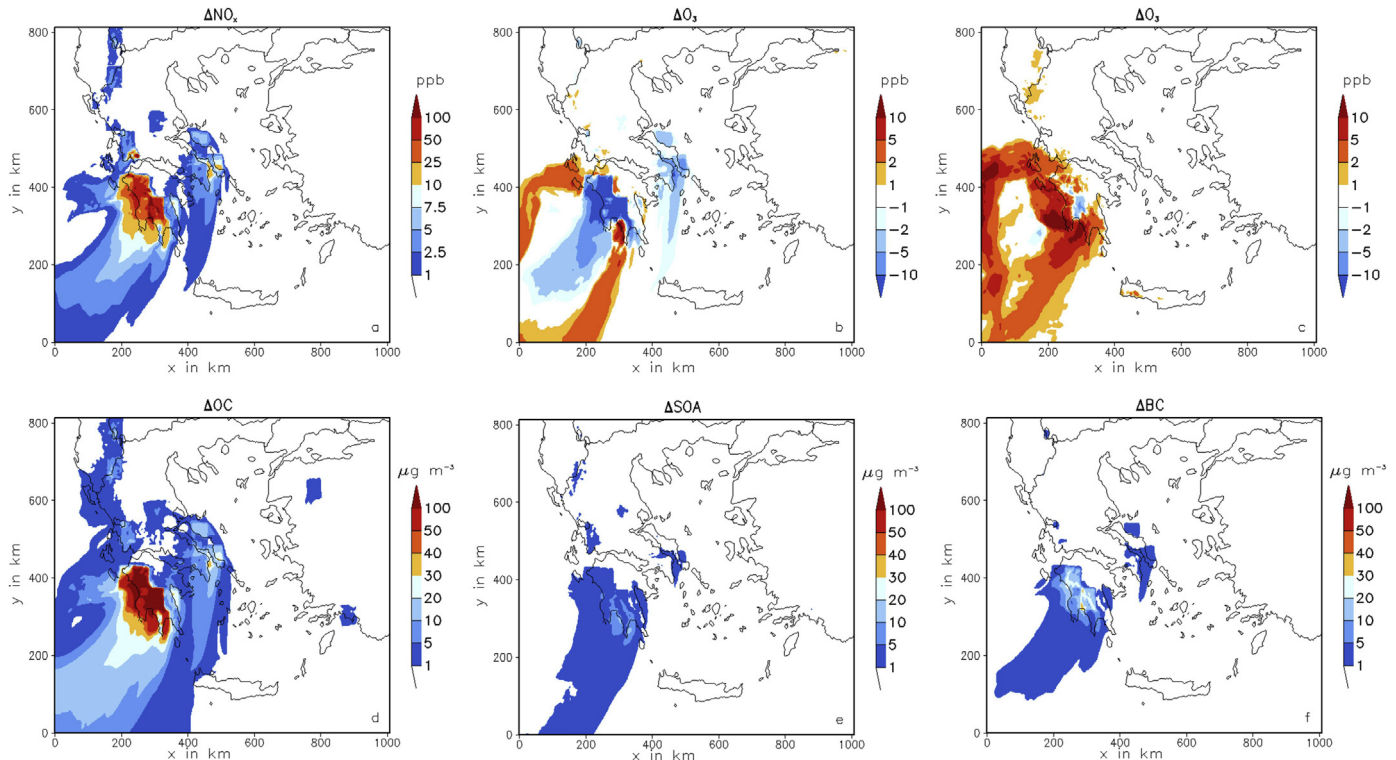


Fig. 5. Spatial distribution of concentration differences (base-case run – scenario 1) of: (a) surface nitrogen oxides (ΔNO_x , ppb), (b) surface ozone (ΔO_3 , ppb), (c) ozone (ΔO_3 , ppb) at the level of 1000 m, (d) organic carbon (ΔOC , $\mu\text{g m}^{-3}$), (e) secondary organic aerosol (ΔSOA , $\mu\text{g m}^{-3}$), and (f) particulate elemental carbon (ΔBC , $\mu\text{g m}^{-3}$), averaged over the peak fire period (25–27 Aug.) of summer 2007.

secondary to total organic components (SOA/OC). In specific, the average OC/EC ratios both in rural/remote (Peloponnese and Euboea, shown in Fig. 6d and e) an urban (Athens, shown in Fig. 6f) areas equal to unity, whereas fire events increase this value up to 11, 8 and 6 respectively. These values are similar to previous observations. During the 2003 intense forest fires in Portugal, the OC/EC ratio was in the range of 4–7 (Pio et al., 2008), while during the

2009 fires in Athens it ranged between 10 and 14 (Amiridis et al., 2012).

On the contrary, SOA/OC ratio during the non-fire period is up to 0.9 for Peloponnese and Euboea and up to 0.6 for Athens (Fig. 6d and f), in accordance to measurements over rural/remote and urban sites, respectively, in the Northern hemisphere (Zhang et al., 2007). This ratio drops down to the extreme value of 0.1 during forest

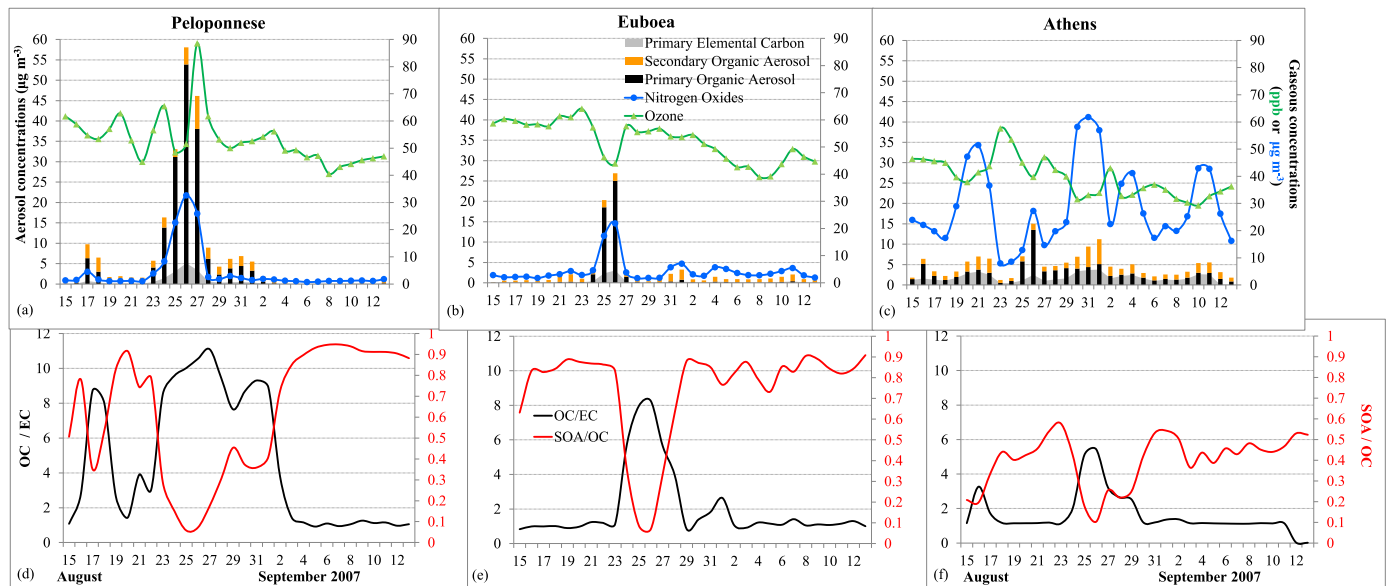


Fig. 6. Temporal variation of gaseous and submicron particle species concentrations (top) and aerosol carbon ratios (bottom) predicted by COSMO-ART at the sites shown in Fig. 1a during 15 August – 13 September, 2007. OC/EC is the organic to elemental carbon and SOA/OC is the secondary to total organics ratio.

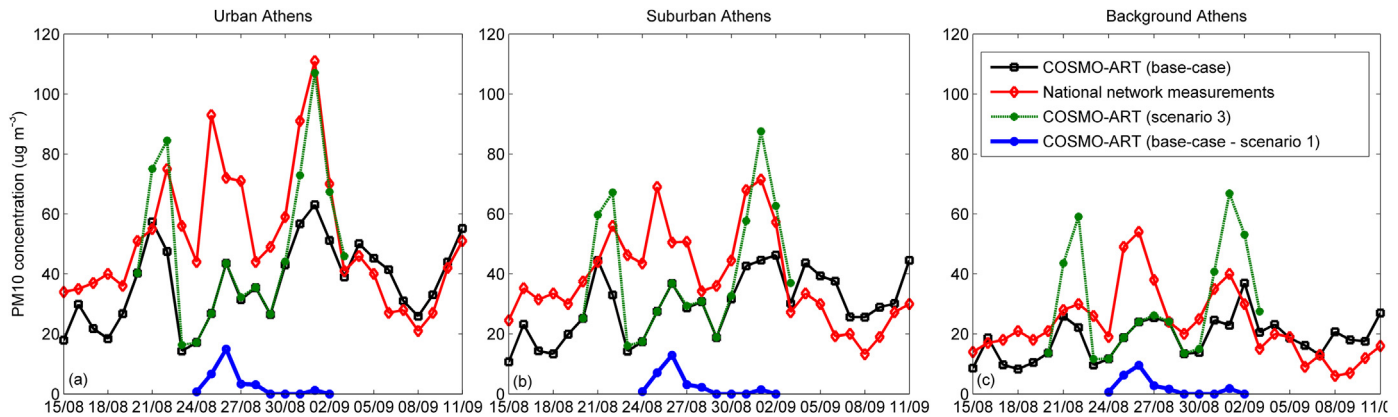


Fig. 7. Temporal variation of ground PM₁₀ concentrations ($\mu\text{g m}^{-3}$) from observations (National Network) and COSMO-ART predictions during 15 August – 13 September 2007, averaged from the: (a) urban, (b) suburban and (c) background sites in Athens, described in Section S6. Base-case and Scenario 3 differences reflect the dust-PM₁₀ mass, while when subtracting scenario 1 from the base-case scenario, the contribution of fires to the total PM₁₀ mass is revealed.

burning, following the fast and high OC production in comparison to the lower oxidation rate towards SOA. It is noted that daily average SOA and EC levels are found stronger influenced by urban pollution (31 Aug.–1 Sept. in Athens) than by wildfires (25–26 Aug. in Athens and Euboea). Nevertheless, SOA formation and evolution in COSMO-ART is not specially treated within the fire plume, and this poses some uncertainties, discussed in the [supplement \(Section S4\)](#).

Secondary inorganic aerosols (sulfates, nitrates and ammonium) are also affected ([Fig. S4](#)) due to the wildfire emissions of their precursors (sulfur dioxide: SO₂, NO_x and ammonia: NH₃). Nevertheless, they are not discussed further, because their increases are small in absolute numbers (3-day-average value up to $+2 \mu\text{g m}^{-3}$), when compared to the aforementioned changes in the carbon aerosol components.

3.4. Influence of wildfires on Athens

Athens is affected by the wildfires of late summer 2007 ignited in Euboea, as indicated in the previous section, and monitored by the Multiangle Imaging SpectroRadiometer of NASA ([Liu et al., 2009](#)). The diurnal variation of the surface particle mass concentrations (PM₁₀) from COSMO-ART predictions as well as from measurements over 3 different types of stations in Athens is presented in [Fig. 7](#). Synergy between model results and measurements bounds PM₁₀ concentrations to specific sources. In particular, in order to quantify the effect of fire plumes over the greater area of Athens, the standard run (black line) is compared to differences from scenario 1 (blue line (in the web version)).

As shown, the fire-induced aerosols account for the 45% of the total surface PM₁₀. This is in line to [Liu et al. \(2009\)](#) findings showing that Euboea fire smoke had an impact on the air quality in Athens comparable with that of local emission sources. The same effect on PM₁₀ concentration over Athens was also calculated for the wildfires of northern Peloponnese during July 2000 ([Lazaridis et al., 2008](#)).

Another pollution episode over Athens occurs on the 1st of September ([Fig. 7](#)). [Liu et al. \(2009\)](#) identified local emissions as the main source of the elevated aerosol concentrations. The current COSMO-ART simulations confirm this finding, although small quantities of fire-induced aerosol are found in Athens. In particular, the Peloponnesian fires are predicted to contribute to this episode around 5% of PM₁₀ mass.

As depicted in [Fig. 7](#), the standard run of COSMO-ART exhibits an overall underestimation of PM₁₀ measurements (red line (in the

web version)). The most important source of discrepancy is the Saharan dust episode, which was not incorporated in this scenario. Nevertheless, the model performance of scenario 3 (green line (in the web version)) captures very nicely the first and the third PM₁₀ spikes (urban values ranging between 80 and 110 $\mu\text{g m}^{-3}$). African dust is not predicted to reach the surface layer during the peak fire period (second spike in the black and green lines (in the web version)).

Monthly mean values together with performance metrics are shown in [Table S2](#). The evaluation criteria used are those established by [Boylan and Russell \(2006\)](#). The mean model performance over Greece is found acceptable. In specific, three sites/cases exhibit good performance, while for the rest of the sites and cases model skill is found average.

It should be noted that raw COSMO-ART outputs for PM_{2.5-10} (non-dust modes) are unrealistically low (below 1 $\mu\text{g m}^{-3}$), which can be regarded as a major factor of PM₁₀ discrepancy. From parallel sampling of PM_{2.5} and PM_{2.5-10} fractions of aerosol in Athens during a year period (March 2008–March 2009), the average PM_{2.5}/PM₁₀ ratio for August was calculated equal to 0.51. To correct for this, PM_{2.5} predictions are divided by this factor to acquire the PM₁₀ values which are compared to observations. An alternative to this simplistic approximation, which will be addressed in the near future, is the incorporation of a road and soil dust production mechanism within COSMO-ART. This model development is expected to significantly improve aerosol model outputs, as shown by previous experimental and modeling studies ([Karanasiou et al., 2009; Athanasopoulou et al., 2010](#)).

Anthropogenic PM_{2.5} predictions for the area of Athens are averaged during the fire (11 $\mu\text{g m}^{-3}$) and the non-fire period (8 $\mu\text{g m}^{-3}$) and then, they are chemically analyzed. Such an analysis complements total aerosol mass observations. Organic aerosol and elemental carbon concentrations during the non-fire period (2.6 $\mu\text{g m}^{-3}$ and 1 $\mu\text{g m}^{-3}$, respectively) are increased by 55% and 33% during the fire period, respectively, composing together the half of the anthropogenic PM_{2.5}. When comparing the hourly values, the maximum of organic aerosols is found much larger during the fire (48 $\mu\text{g m}^{-3}$, at the urban station on August 26, 20:00 UTC) than during the non-fire period (12 $\mu\text{g m}^{-3}$, at a suburban station on August 21, 20:00 UTC). Elemental carbon is moderately increased (8 $\mu\text{g m}^{-3}$ and 6 $\mu\text{g m}^{-3}$, respectively), while the maximum concentrations of the rest species (sulfates, nitrates, ammonium) do not occur during the fire event.

3.5. Radiative and temperature impact of wildfires

During the peak fire period, particles exert an important impact on the radiation budget over and downwind Peloponnese (Fig. 8). The figure presents the simulated averages (25–27 Aug., 2007) and the actual values at 26 Aug., 1200 UTC, when the largest differences in temperature occurred.

The average short-wave radiative forcing at the surface is negative, reaches -20 (-50) W m^{-2} (values in brackets give the results for 26 Aug., 1200 UTC) over the fire spots and decreases from -5 to -20 (from -10 to -50) W m^{-2} downwind. The spatial pattern of the reduction of solar energy reaching the ground, closely follows the AOD spatial pattern (Fig. 3f). There is also a positive forcing due to the effect of the fire plume on the net upward long-wave flux, though weaker (3-day-average value up to $+10 \text{ W m}^{-2}$). Hence, the net radiative forcing of wildfires is negative and around -10 W m^{-2} over the burning area of Peloponnese. Radiative cooling at the top of the atmosphere exhibits the same spatial distribution, but compared to the radiative forcing at the surface its values are halved. This modification of the radiative fluxes due to the aerosols modifies the diabatic heating of the atmosphere. During the fire episode the resulting feedbacks lead to a cooling of the air up to -0.5 (-5) K at 2 m above surface (Fig. 8c).

Wildfire effects on radiation were previously studied with the use of models for the area of Russia during August 2010 (Péré et al., 2014) and for Asia during April 2008 (Natarajan et al., 2012). Both

studies calculated daily average radiation decreases much higher than aforementioned (up to -50 and -150 W m^{-2} , respectively). Nevertheless, aerosol loadings caused by these two fire events were calculated much more intense than these from the Peloponnesian fires. In specific, AOD values over fire spots in Russia and Asia were well above 2, while AOD calculations from the current study are up to 1.2 (Fig. 3). The feedback on near-surface air temperature was calculated only for the fire case in Russia and estimated, as expected, higher than in this study (up to -2.6°C in diurnal averages).

Near-surface air temperature depends not only on incident solar flux, but also on sensible and latent heat fluxes, aerosol absorption near the ground and atmospheric circulation. Hence, the resulting effect of these different mechanisms on the 2 m temperature can vary from one region to another, as previously shown by Zanis (2009) over Europe. In the case studied here, a warming effect (up to $+1 \text{ K}$) of biomass burning aerosol at the surface over sea at 26 Aug., 1200 UTC (Fig. 8d) is found. In the following we will explain this -at a first glance surprising- warming over sea and compare it with the cooling over land.

For a better understanding of this different behavior, Fig. 9 shows the vertical profiles of the concentration of pure and coated (aged) soot at a grid point above land and above sea, respectively. The corresponding temperature profiles for the cases with and without biomass burning aerosol are also shown. At the land surface, the reduction of short wave radiation leads to a decrease of surface temperature of up to 5 K (hourly value). This

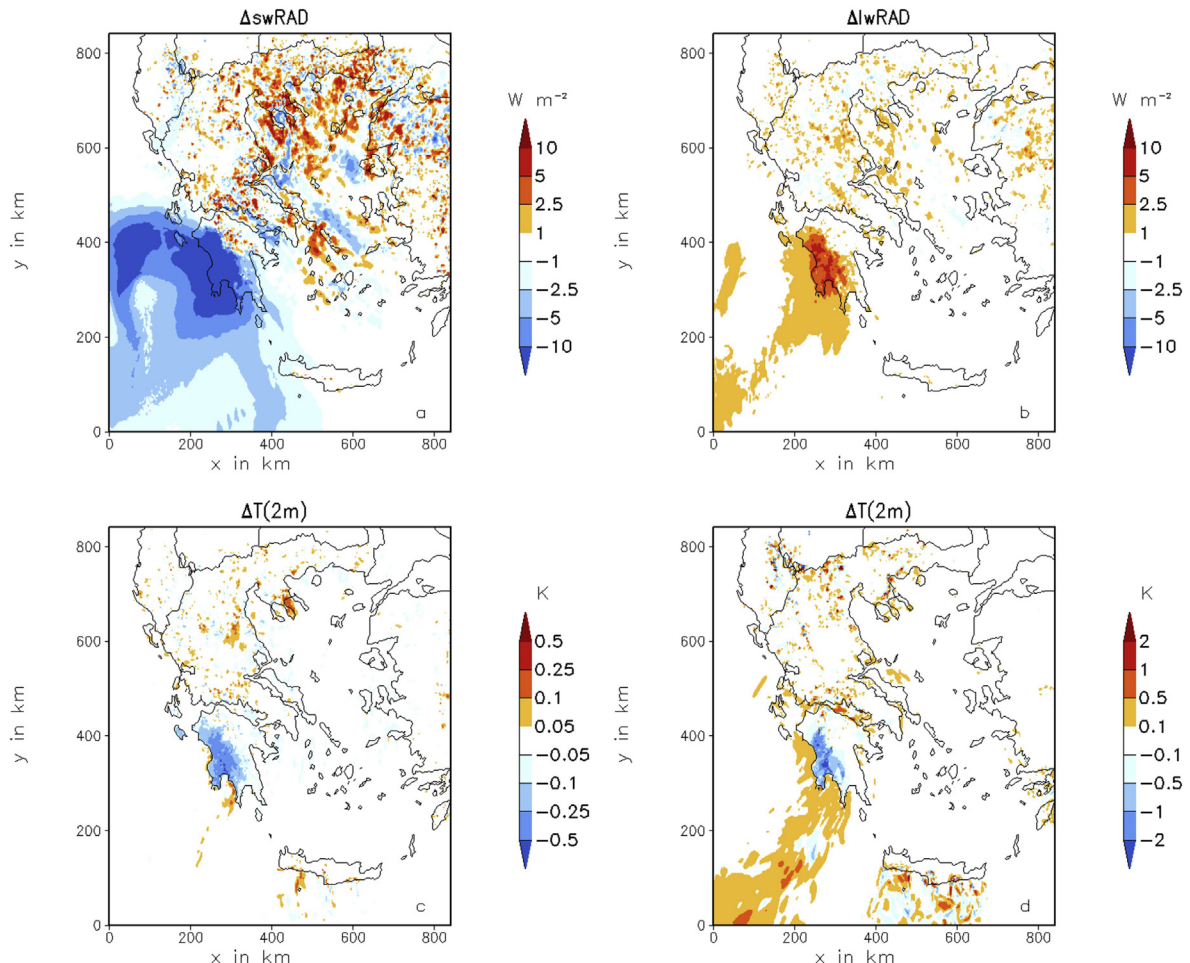


Fig. 8. Spatial distribution of differences (base-case scenario – scenario 1) of: (a) short-wave surface radiation (in W m^{-2}), (b) long-wave surface radiation (in W m^{-2}), (c) air temperature at 2 m (in K), averaged over the peak fire period (25–27 Aug.) of summer 2007. (d) air temperature at 26 Aug., 1200 UTC at 2 m (in K).

temperature decrease reaches up to a height of about 1 km above surface. The grid point above sea shows an increase of temperature by up to 2 K throughout the boundary layer, although shortwave radiation is reduced by the biomass burning aerosol. As the sea surface is kept constant, which is a reasonable assumption due to the high heat capacity of water, the reduction of short wave radiation is not followed by a temperature decrease. Moreover, the absorption by soot, which is amplified when soot particles have a soluble shell (coated), leads to a remarkable increase in temperature when biomass burning aerosol is accounted for. Above land and above sea, the absorbing aerosol leads to a stabilization of the atmosphere. This is an important finding as by this stabilization the turbulent mixing is reduced within the plume. This effect is even stronger above sea. The biomass burning aerosol creates its own mixing environment. Hence it is estimated that the effect of reduced vertical mixing above sea is responsible for the fact that the biomass burning plume is traveling such a long distance towards Africa (1000 km), as seen in the satellite image (Fig. 1b).

To study the effect of the direct heat input of wildfires at Peloponnese on air temperature we carried out an additional model run (scenario 2). We found a small heat input caused by the Peloponnese fires, which modified temperature in the order of mK. Overall, the modification of the radiative fluxes by the biomass burning aerosol during the simulated situation leads to a

remarkable modification of the near surface temperature over land, to a warming of the boundary layer over sea, and to a thermal stabilization of the atmosphere. These effects are much greater than the almost negligible temperature changes due to the direct heat input by the vegetation fires.

4. Conclusions

This is to our knowledge the first holistic study of a severe wildfire event in Europe. The high resolution application of the COSMO-ART model over Greece enabled the concurrent assessment of fire danger conditions, air quality and aerosol radiative forcing during the most striking fire episode of 2007 in the Mediterranean area.

The significant role of meteorological conditions in fire ignition and the adequate reproduction of the increased fire risk by model predictions (FWI above 50) show the necessity of incorporating FWI estimates in the national meteorological forecasts and early warning systems for fire prevention.

This is a synergistic study so that model outputs complement observations on identifying four different aerosol conditions over the eastern Mediterranean. AOD maximum values (1–1.2) occur during the African dust intrusion. Type-dependent AOD predictions show that these loadings are a mixture of dust, sea-salt and

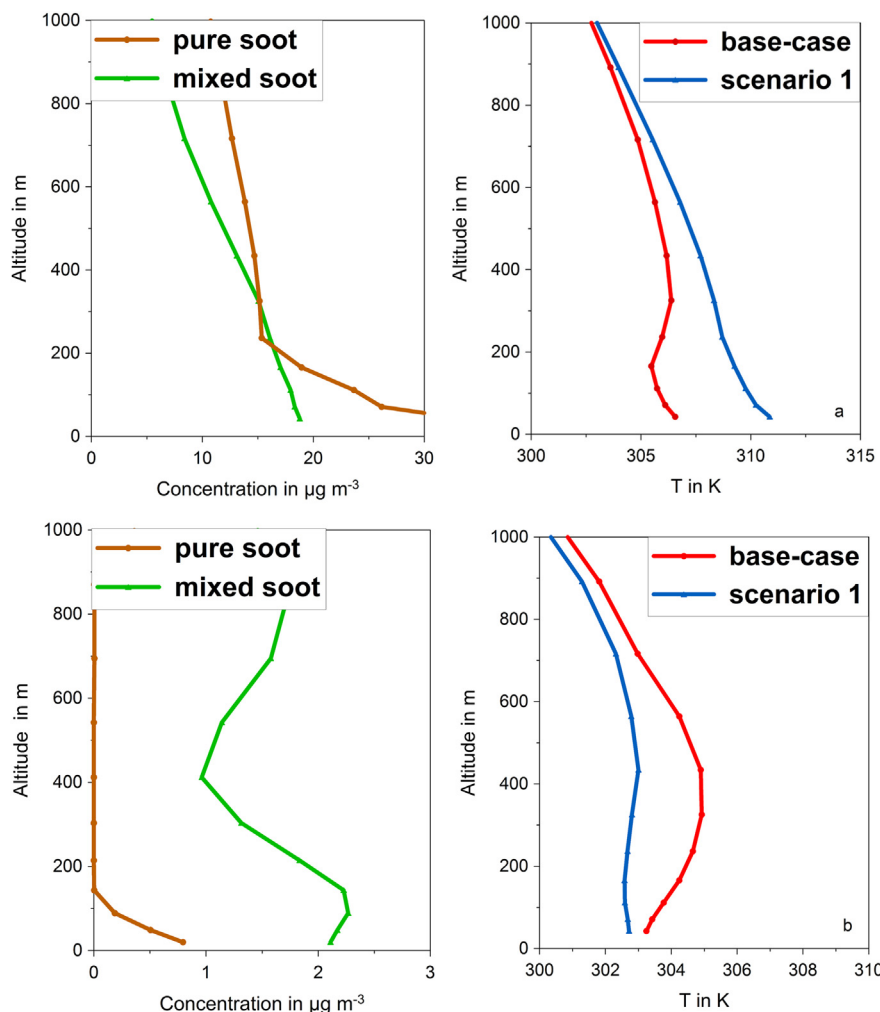


Fig. 9. Vertical concentration profiles of pure soot particles (brown lines), mixed (aged) soot (green lines), temperature of the base-case scenario (red lines) and from the scenario 1 (blue lines); (a) over land, (b) over water. Results are presented for 26 Aug. 2007, 1200 UTC. (For interpretation of the references to colour in this figure legend, the reader is referred to the web version of this article.)

anthropogenic aerosol. Forest burning over Peloponnese results to three times higher AOD values (0.75–1) than aerosol loads before fires ignite. Anthropogenic pollution over northern Greece and northwestern Turkey shapes somewhat lower AOD values (around 0.65).

Compared to the non-fire period, OC over Athens raised five times (daily average value of $15 \mu\text{g m}^{-3}$), and OC/EC ratio increased from 1 to 6 during the fire period. In parallel, the SOA/OC ratio decreased from 0.6 to 0.1. These values refer to the first pollution episode over Athens (24–26 August), when the fire plume from Euboea contributes around 45% to the total PM₁₀ concentrations. During the second pollution episode (31 August – 1 September), fire plumes affect PM₁₀ concentrations over Athens only by 5%.

The radiative impact of the changes in OC, aerosol water and black carbon aerosols triggered by the Peloponnesian fire events is negative (3-day-average value -10 W m^{-2}), causing an air cooling of -0.5 K . The warming effect from the direct heat input is found lower more than 2 orders of magnitude, thus the net temperature changes caused in the greater area of the wildfires are negative. However, temperature increases are found offshore (hourly value up to $+2 \text{ K}$), due to the amplified radiation absorption by coated (aged) soot coupled to the intense stabilization of the atmosphere above the sea surface. The latter causes a reduced vertical mixing, responsible for the high spatial extent (1000 km) of this fire plume. These findings support that the wildfire radiative effects should be accounted for in numerical weather forecast.

The current study presents an extensive model evaluation over the eastern Mediterranean. Thus, apart from proving the model's competence to reproduce the meteorological and aerosol situation over the area, it also revealed model deficiencies, which serve as challenges for future model development. In specific, coarse aerosol concentrations are found strongly underestimated. Thus, the soil erosion and road dust production mechanisms should be incorporated into COSMO-ART, so as to improve its competence under the climatic conditions (high temperatures and low humidity) of the southern Europe.

The weather conditions during the wildfire period of late summer 2007 in Greece have already been assessed as a typical summertime meteorological regime during the latter part of the century (Founda and Giannakopoulos, 2009). Therefore, the chemical and radiative forcing estimates of the current study cannot only be viewed as the highest in southern Europe during the last decade, but also as representative of a fire event likely to occur in the future.

Acknowledgments

This work was partly supported by the CLIM-RUN project (www.climrun.eu, grant agreement no: 265192), funded under the European Commission's (EU) Seventh Framework Programme (FP7). E. Athanasopoulou would like to acknowledge support from the project AERAS-EtS (within the framework of the Action «Supporting Postdoctoral Researchers» of the Operational Program “Education and Lifelong Learning”, co-financed by the European Social Fund (ESF) and the Greek State). A. Karali and C. Giannakopoulos would like to acknowledge support from the project XENIOS (no 09COP-31-867) financed by the EU (ERDF) and Greek national funds through the Operational Program “Competitiveness and Entrepreneurship” of the National Strategic Reference Framework (NSRF) Research Funding Program COOPERATION 2009. Analyses and visualizations of the satellite images used in this article were produced with the Giovanni online data system, developed and maintained by the NASA GES DISC. We acknowledge the mission scientists and Principal Investigators who provided the data used in this research effort. The Barcelona Supercomputing Center (<http://www.bsc.es/projects/earthscience/BSC-DREAM/>) is also acknowledged for the provision of data from the BSC-DREAM8b (Dust REgional Atmospheric Model) model.

Appendix A. Supplementary data

Supplementary data related to this article can be found at <http://dx.doi.org/10.1016/j.atmosenv.2014.05.077>.

References

- Amiridis, V., Zerefos, C., Kazadzis, S., Gerasopoulos, E., Eleftheratos, K., Vrekoussis, M., Stohl, A., Mamouri, R.E., Kokkalis, P., Papayannis, A., Eleftheriadis, K., Diapouli, E., Keramitsoglou, I., Kontoes, C., Kotroni, V., Lagouvardos, K., Marinou, E., Giannakaki, E., Kostopoulou, E., Giannakopoulos, C., Richter, A., Burrows, J.P., Mihalopoulos, N., 2012. Impact of the 2009 Attica wild fires on the air quality in urban Athens. *Atmos. Environ.* 46, 536–544.
- Athanasiopoulou, E., Tombrou, M., Russell, A.G., Karanasiou, A., Eleftheriadis, K., Dandou, A., 2010. Implementation of road and soil dust emission parameterizations in the aerosol model CAMx: applications over the greater Athens urban area affected by natural sources. *J. Geophys. Res. Atmos.* 115.
- Athanasiopoulou, E., Vogel, H., Vogel, B., Tsimpidi, A.P., Pandis, S.N., Knote, C., Fountoukis, C., 2013. Modeling the meteorological and chemical effects of secondary organic aerosols during an EUCAARI campaign. *Atmos. Chem. Phys.* 13, 625–645.
- Baldauf, M., Seifert, A., Förstner, J., Majewski, D., Raschendorfer, M., Reinhardt, T., 2011. Operational convective-scale numerical weather prediction with the COSMO model: description and sensitivities. *Mon. Weather Rev.* 139, 3887–3905.
- Bangert, M., Kottmeier, C., Vogel, B., Vogel, H., 2011. Regional scale effects of the aerosol cloud interaction simulated with an online coupled comprehensive chemistry model. *Atmos. Chem. Phys.* 11, 4411–4423.
- Basart, S., Pérez, C., Nickovic, S., Cuevas, E., Baldasano, J.M., Baldasano, J.M., Baldasano, J.M., Baldasano, J.M., Baldasano, J.M., Baldasano, J.M., 2012. Development and Evaluation of the BSC-DREAM8b Dust Regional Model Over Northern Africa, the Mediterranean and the Middle East [WWW Document].
- Bassi, S., Kettunen, M., Kampa, E., Cavalieri, S., 2008. Forest Fires: Causes and Contributing Factors in Europe. IP/A/ENVI/ST/2007-15, PE 401.003.
- Bossioli, E., Tombrou, M., Karali, A., Dandou, A., Paronis, D., Sofiev, M., 2012. Ozone production from the interaction of wildfire and biogenic emissions: a case study in Russia during spring 2006. *Atmos. Chem. Phys.* 12, 7931–7953.
- Boylan, J.W., Russell, A.G., 2006. PM and light extinction model performance metrics, goals, and criteria for three-dimensional air quality models. *Atmos. Environ.* 40, 4946–4959.
- Bytherowicz, A., 2009. Wildland Fires and Air Pollution. Elsevier.
- Carvalho, A., Flannigan, M.D., Logan, K., Miranda, A.I., Borrego, C., 2008. Fire activity in Portugal and its relationship to weather and the Canadian fire weather index system. *Int. J. Wildland Fire* 17, 328–338.
- Doms, G., Schaeftler, U., Baldauf, M., 2011. A Description of the Nonhydrostatic Regional COSMO-Model Part I: Dynamics and Numerics. COSMO-Model 4.20, Printed at Deutscher Wetterdienst, P.O. Box 100465, 63004 Offenbach, (Germany).
- Emmons, L.K., Walters, S., Hess, P.G., Lamarque, J.-F., Pfister, G.G., Fillmore, D., Granier, C., Guenther, A., Kinnison, D., Laepple, T., Orlando, J., Tie, X., Tyndall, G., Wiedinmyer, C., Baughcum, S.L., Kloster, S., 2010. Description and evaluation of the model for ozone and related chemical tracers, version 4 (MOZART-4). *Geosci. Model Dev.* 3, 43–67.
- Engelstaedter, S., Washington, R., 2007. Atmospheric controls on the annual cycle of North African dust. *J. Geophys. Res. Atmos.* 112.
- EU, European Union, 2001. Report No 1: Forest Fires in Southern Europe. Belgium, European Commission, Brussels, p. 45.
- European Commission, 2008. Forest Fires in Europe 2007 Fire Campaign. European Communities, Italy.
- FAO Food and Agriculture Organization, 2007. Fire management – Global assessment 2006. FAO Forestry Paper No. 151 Rome, Italy, p. 121.
- Founda, D., Giannakopoulos, C., 2009. The exceptionally hot summer of 2007 in Athens, Greece – A typical summer in the future climate? *Glob. Planet. Change* 67, 227–236.
- Gerasopoulos, E., Amiridis, V., Kazadzis, S., Kokkalis, P., Eleftheratos, K., Andreae, M.O., Andreae, T.W., El-Askary, H., Zerefos, C.S., 2011. Three-year ground based measurements of aerosol optical depth over the Eastern Mediterranean: the urban environment of Athens. *Atmos. Chem. Phys.* 11, 2145–2159.
- Hodnebrog, Ø., Solberg, S., Stordal, F., Svennby, T.M., Simpson, D., Gauss, M., Hilboll, A., Pfister, G.G., Turquety, S., Richter, A., Burrows, J.P., Denier van der Gon, H.A.C., 2012. Impact of forest fires, biogenic emissions and high temperatures on the elevated Eastern Mediterranean ozone levels during the hot summer of 2007. *Atmos. Chem. Phys.* 12, 8727–8750.
- Hodzic, A., Madronich, S., Bohn, B., Massie, S., Menut, L., Wiedinmyer, C., 2007. Wildfire particulate matter in Europe during summer 2003: meso-scale

- modeling of smoke emissions, transport and radiative effects. *Atmos. Chem. Phys.* 7, 4043–4064.
- Iliadis, L.S., Papastavrou, A.K., Lefakis, P.D., 2002. A computer-system that classifies the prefectures of Greece in forest fire risk zones using fuzzy sets. *For. Policy Econ.* 4, 43–54.
- Israelevich, P.L., Levin, Z., Joseph, J.H., Ganor, E., 2002. Desert aerosol transport in the Mediterranean region as inferred from the TOMS aerosol index. *J. Geophys. Res. Atmos.* 107, AAC 13–21–AAC 13–13.
- Jin, Y., Randerson, J.T., Goudelis, M.L., Goetz, S.J., 2012. Post-fire changes in net shortwave radiation along a latitudinal gradient in boreal North America: fire-induced latitudinal surface forcing. *Geophys. Res. Lett.* 39.
- Karali, A., Hatzaki, M., Giannakopoulos, C., Roussos, A., Xanthopoulos, G., Tenentes, V., 2014. Sensitivity and evaluation of current fire risk and future projections due to climate change: the case study of Greece. *Nat. Hazards Earth Syst. Sci.* 14, 143–153.
- Karanasiou, A.A., Siskos, P.A., Eleftheriadis, K., 2009. Assessment of source apportionment by positive matrix factorization analysis on fine and coarse urban aerosol size fractions. *Atmos. Environ.* 43, 3385–3395.
- Kouvarakis, G., Vrekoussis, M., Mihalopoulos, N., Kourtidis, K., Rappenglueck, B., Gerasopoulos, E., Zerefos, C., 2002. Spatial and temporal variability of tropospheric ozone (O_3) in the boundary layer above the Aegean Sea (eastern Mediterranean). *J. Geophys. Res. Atmos.* 107, PAU 4–1–PAU 4–14.
- Kuenen, J., Denier van der Gon, H., Visschedijk, A., van der Brugh, H., 2011. High Resolution European Emission Inventory for the Years 2003–2007. TNO-report TNO-060-UT-2011–00588, Utrecht, 2011.
- Lazaridis, M., Latos, M., Aleksandropoulou, V., Hov, Ø., Papayannis, A., Tørseth, K., 2008. Contribution of forest fire emissions to atmospheric pollution in Greece. *Air Qual. Atmos. Health* 1, 143–158.
- Liu, Y., Kahn, R.A., Chaloulakou, A., Kourakis, P., 2009. Analysis of the impact of the forest fires in August 2007 on air quality of Athens using multi-sensor aerosol remote sensing data, meteorology and surface observations. *Atmos. Environ.* 43, 3310–3318.
- Lundgren, K., Vogel, B., Vogel, H., Kottmeier, C., 2013. Direct radiative effects of sea salt for the Mediterranean region under conditions of low to moderate wind speeds: DRE of sea salt for the mediterranean. *J. Geophys. Res. Atmos.* 118, 1906–1923.
- Märtensson, E.M., Nilsson, E.D., de Leeuw, G., Cohen, L.H., Hansson, H.-C., 2003. Laboratory simulations and parameterization of the primary marine aerosol production. *J. Geophys. Res. Atmos.* 108.
- Martins, V., Miranda, A.I., Carvalho, A., Schaap, M., Borrego, C., Sá, E., 2012. Impact of forest fires on particulate matter and ozone levels during the 2003, 2004 and 2005 fire seasons in Portugal. *Sci. Total Environ.* 414, 53–62.
- Mc Arthur, A.G., 1967. Fire Behaviour in Eucalypt Forests, Department of National Development, Forestry and Timber Bureau Leaflet No.107, Canberra, Australia.
- Moriondo, M., Good, P., Durao, R., Bindi, M., Giannakopoulos, C., CorteReal, J., 2006. Potential impact of climate change on fire risk in the Mediterranean area. *Clim. Res.* 31, 85–95.
- Natarajan, M., Pierce, R.B., Schaack, T.K., Lenzen, A.J., Al-Saadi, J.A., Soja, A.J., Charlock, T.P., Rose, F.G., Winker, D.M., Worden, J.R., 2012. Radiative forcing due to enhancements in tropospheric ozone and carbonaceous aerosols caused by Asian fires during spring 2008. *J. Geophys. Res. Atmos.* 117.
- Ovadnevaite, J., Manders, A., de Leeuw, G., Monahan, C., Ceburnis, D., O'Dowd, C.D., 2013. A sea spray aerosol flux parameterization encapsulating wave state. *Atmos. Chem. Phys. Discuss.* 13, 23139–23171.
- Péré, J.C., Bessagnet, B., Mallet, M., Waquet, F., Chiapello, I., Minvielle, F., Pont, V., Menut, L., 2014. Direct radiative effect of the Russian wildfires and its impact on air temperature and atmospheric dynamics during August 2010. *Atmos. Chem. Phys.* 14, 1999–2013.
- Pereira, J.S., Correia, A.V., Correia, A.P., Branco, M., Bugallo, M., Caldeira, M.C., Cruz, C.S., Freitas, H., Oliveira, A.C., Pereira, J.M.C., Reis, R.M., Vasconcelos, M.J., 2002. Forests and biodiversity. In: Santos, F.D., Forbes, K., Moita, R. (Eds.), *Climate Change in Portugal: Scenarios, Impacts and Adaptation Measures*. Gravida, Lisbon), pp. 363–413.
- Pérez, C., Nickovic, S., Baldasano, J.M., Sicard, M., Rocadenbosch, F., Cachorro, V.E., 2006a. A long Saharan dust event over the western Mediterranean: Lidar, Sun photometer observations, and regional dust modeling. *J. Geophys. Res. Atmos.* 111.
- Perez, Nickovic, S., Pejanovic, G., Baldasano, J.M., Özsoy, E., 2006b. Interactive Dust-radiation Modeling: a Step to Improve Weather Forecasts [WWW Document].
- Pio, C.A., Legrand, M., Alves, C.A., Oliveira, T., Afonso, J., Caseiro, A., Puxbaum, H., Sanchez-Ochoa, A., Gelencsér, A., 2008. Chemical composition of atmospheric aerosols during the 2003 summer intense forest fire period. *Atmos. Environ.* 42, 7530–7543.
- Poupkou, A., Markakis, K., Liora, N., Giannaros, T.M., Im, U., Daskalakis, N., Myriokefalitakis, S., Melas, D., Zanis, P., Kanakidou, M., Zerefos, C.S., 2013. Study of the impact of an intense biomass burning event on the air quality in the Eastern Mediterranean. In: Helmis, C.G., Nastos, P.T. (Eds.), *Advances in Meteorology, Climatology and Atmospheric Physics*, Springer Atmospheric Sciences. Springer Berlin Heidelberg, pp. 1189–1195.
- San-Miguel-Ayanz, J., Moreno, J.M., Camia, A., 2013. Analysis of large fires in European Mediterranean landscapes: lessons learned and perspectives. *For. Ecol. Manag.* 294, 11–22.
- Sifakis, N.I., Iossifidis, C., Kontoes, C., Keramitsoglou, I., 2011. Wildfire detection and tracking over Greece using MSG-SEVIRI satellite data. *Remote Sens.* 3, 524–538.
- Strada, S., Mari, C., Filippi, J.-B., Bosseur, F., 2012. Wildfire and the atmosphere: modelling the chemical and dynamic interactions at the regional scale. *Atmos. Environ.* 51, 234–249.
- Van der Werf, G.R., Randerson, J.T., Giglio, L., Collatz, G.J., Mu, M., Kasibhatla, P.S., Morton, D.C., DeFries, R.S., Jin, Y., van Leeuwen, T.T., 2010. Global fire emissions and the contribution of deforestation, savanna, forest, agricultural, and peat fires (1997–2009). *Atmos. Chem. Phys.* 10, 11707–11735.
- Van Wagner, C.E., 1987. Development and Structure of the Canadian Forest Fire Weather Index System 35.
- Venäläinen, A., Heikinheimo, M., 2003. The Finnish Forest Fire Index Calculation System. In: Zschau, P.D.J., Küppers, A. (Eds.), *Early Warning Systems for Natural Disaster Reduction*. Springer Berlin Heidelberg, pp. 645–647.
- Vogel, B., Vogel, H., Bäumer, D., Bangert, M., Lundgren, K., Rinke, R., Stanelle, T., 2009. The comprehensive model system COSMO-ART – radiative impact of aerosol on the state of the atmosphere on the regional scale. *Atmos. Chem. Phys.* 9, 8661–8680.
- Zanis, P., 2009. A study on the direct effect of anthropogenic aerosols on near surface temperature over Southeastern Europe during summer 2000 based on regional climate modelling. *Ann. Geophys.* 27, 3977–3988.
- Zhang, Q., Jimenez, J.L., Canagaratna, M.R., Allan, J.D., Coe, H., Ulbrich, I., Alfarra, M.R., Takami, A., Middlebrook, A.M., Sun, Y.L., Dzepina, K., Dunlea, E., Docherty, K., DeCarlo, P.F., Salcedo, D., Onasch, T., Jayne, J.T., Miyoshi, T., Shimono, A., Hatakeyama, S., Takegawa, N., Kondo, Y., Schneider, J., Drewnick, F., Borrmann, S., Weimer, S., Demerjian, K., Williams, P., Bower, K., Bahreini, R., Cottrell, L., Griffin, R.J., Rautiainen, J., Sun, J.Y., Zhang, Y.M., Worsnop, D.R., 2007. Ubiquity and dominance of oxygenated species in organic aerosols in anthropogenically-influenced Northern Hemisphere midlatitudes. *Geophys. Res. Lett.* 34.